Silica-Like Malleable Materials from Permanent Organic Networks

Damien Montarnal, *et al.*

Science **334**, 965 (2011);
DOI: 10.1126/science.1212648

distinct length scales, we demonstrated the emergence of entirely different mechanical properties. In addition to possible applications for an ultralight material with high energy absorption and recoverability, we anticipate that these results will help reshape our understanding of the interaction between material properties and structural architecture.

References and Notes

1. Guinness Book of World Records, Least Dense Solid (2003), www.guinnessworldrecords.com/records-1/least-dense-solid/.
2. T. M. Tillotson, L. W. Hrubesh, *J. Non-Cryst. Solids* **145**, 44 (1992).
3. J. Zou *et al*., *ACS Nano* **4**, 7293 (2010).
4. A. Verdooren, H. M. Chan, J. L. Grenestedt, M. P. Harmer, H. S. Caram, *J. Am. Ceram. Soc.* **89**, 3101 (2006).
5. B. C. Tappan *et al*., *J. Am. Chem. Soc.* **128**, 6589 (2006).
6. M. Chanda, S. K. Roy, *Plastics Technology Handbook* (CRC Press, Boca Raton, FL, 2007).
7. B. A. S. F. Corporation, Materials Safety Data Sheet for Basotect V3012 (2007), www.basf.co.kr/02_products/01_thermoplastics/spe/document/MSDS-Basotect%20V3012.pdf.
8. L. J. Gibson, M. F. Ashby, *Cellular Solids: Structure and Properties* (Cambridge Univ. Press, Cambridge, 1997).
9. H.-S. Ma, J.-H. Prévost, R. Jullien, G. W. Scherer, *J. Non-Cryst. Solids* **285**, 216 (2001).
10. R. S. Lakes, *Nature* **361**, 511 (1993).
11. A. J. Jacobsen, W. Barvosa-Carter, S. Nutt, *Acta Mater.* **55**, 6724 (2007).
12. A. J. Jacobsen, W. Barvosa-Carter, S. Nutt, *Adv. Mater.* **19**, 3892 (2007).
13. A. J. Jacobsen, W. Barvosa-Carter, S. Nutt, *Acta Mater.* **56**, 2540 (2008).
14. S. H. Park, D. N. Lee, *J. Mater. Sci.* **23**, 1643 (1988).
15. S. Y. Chang, Y. S. Lee, H. L. Hsiao, T. K. Chang, *Metall. Mater. Trans. A* **37A**, 2939 (2006).
16. J. Lian *et al*., *Nano Lett.* **11**, 4118 (2011).
17. G. F. Lee, B. Hartmann, *J. Sound Vibrat.* **211**, 265 (1998).
18. M. F. Ashby *et al*., *Metal Foams: A Design Guide* (Butterworth-Heinemann, Burlington, MA, 2000), p. 43.
19. N. J. Mills, *Cell. Polym.* **5**, 293 (2006).
20. A. Cao, P. L. Dickrell, W. G. Sawyer, M. N. Ghasemi-Nejhad, P. M. Ajayan, *Science* **310**, 1307 (2005).
21. J. R. Trelewicz, C. A. Schuh, *Acta Mater.* **55**, 5948 (2007).
22. J. Gross, T. Schlief, J. Fricke, *Mater. Sci. Eng. A* **168**, 235 (1993).
23. M. A. Worsley, S. O. Kucheyev, J. H. Satcher Jr., A. V. Hamza, T. F. Baumann, *Appl. Phys. Lett.* **94**, 073115 (2009).
24. V. S. Deshpande, N. A. Fleck, M. F. Ashby, *J. Mech. Phys. Solids* **49**, 1747 (2001).
25. V. S. Deshpande, M. F. Ashby, N. A. Fleck, *Acta Mater.* **49**, 1035 (2001).
26. V. S. Deshpande, N. A. Fleck, *Int. J. Solids Struct.* **38**, 6275 (2001).
27. L. J. Gibson, M. F. Ashby, *Proc. R. Soc. London Ser. A* **382**, 43 (1982).
28. Hexcel Corporation, *HexWeb Honeycomb Attributes and Properties* (1999); datasheet available at www.hexcel.com/Resources/DataSheets/Brochure-Data-Sheets/Honeycomb_Attributes_and_Properties.pdf.
29. M. Moner-Girona, A. Roig, E. Molins, E. Martinez, J. Esteve, *Appl. Phys. Lett.* **75**, 653 (1999).

Acknowledgments: The authors gratefully acknowledge the financial support by Defense Advanced Research Projects Agency under the Materials with Controlled Microstructural Architecture program managed by J. Goldwasser (contract no. W91CRB-10-0305) and thank J. W. Hutchinson and C. S. Roper for useful discussions. A patent application regarding the structure and formation process of the ultralight microlattices has been submitted to the U.S. Patent and Trademark Office. The polymer waveguide process has been patented (U.S. Patent 7,382,959, U.S. Patent 7,653,279, and U.S. Patent 8,017,193), but the template can be fabricated in other ways.

Supporting Online Material

www.sciencemag.org/cgi/content/full/334/6058/962/DC1
Materials and Methods
Fig. S1
Table S1
References
Movie S1

25 July 2011; accepted 12 October 2011
10.1126/science.1211649

Silica-Like Malleable Materials from Permanent Organic Networks

Damien Montarnal, Mathieu Capelot, François Tournilhac, Ludwik Leibler*

Permanently cross-linked materials have outstanding mechanical properties and solvent resistance, but they cannot be processed and reshaped once synthesized. Non–cross-linked polymers and those with reversible cross-links are processable, but they are soluble. We designed epoxy networks that can rearrange their topology by exchange reactions without depolymerization and showed that they are insoluble and processable. Unlike organic compounds and polymers whose viscosity varies abruptly near the glass transition, these networks show Arrhenius-like gradual viscosity variations like those of vitreous silica. Like silica, the materials can be wrought and welded to make complex objects by local heating without the use of molds. The concept of a glass made by reversible topology freezing in epoxy networks can be readily scaled up for applications and generalized to other chemistries.

Thermoset polymers such as Bakelite must be polymerized in a mold having the shape of the desired object because once the reaction is completed, the polymer cannot be reshaped or reprocessed by heat or with solvent. In contrast, thermoplastics, when heated, can flow, which permits extrusion, injection, and molding of objects. Depending on the chemical nature of the plastic, during cooling, solidification occurs by crystallization or by glass transition. During vitrification, as the temperature is lowered below the glass transition, the viscosity abruptly increases in a narrow temperature range, and the material becomes so viscous that it behaves essentially like a solid with an elastic modulus of about 10^9 to 10^{10} Pa (*1*). Nevertheless, compared to processable plastics, cross-linked polymers have superior dimensional stability; have high-temperature mechanical, thermal, and environmental resistance; and are irreplaceable in many demanding applications, such as in the aircraft industry. High-performance coatings, adhesives, rubbers, light-emitting diode lenses, and solar cell encapsulants are made of permanently cross-linked polymer networks as well.

Making covalent links reversible could provide a way to combine processability, reparability, and high performance (*2*–*6*). Networks with bonds able to break and reform (*7*–*9*) or to exchange pairs of atoms (*10*) can relax stresses and flow. The challenge is to allow rapid reversible reactions at high temperatures or by a convenient stimulus and to fix the network at service conditions. In this context, cleavage or exchange reactions by addition-fragmentation in the presence of radicals offer interesting possibilities (*5*, *11*–*14*). Scott *et al*. demonstrated photoinduced plasticity in cross-linked polymers (*11*). Similarly, reparability and self-healing can be induced either thermally (*13*) or photochemically (*15*, *16*) in radical systems. However, these systems undergo unavoidable termination reactions that limit reversibility of the networks.

In parallel, a completely different concept based on chemical equilibrium between bond breaking and reforming without irreversible side reactions has been developed (*17*–*20*). In these systems, heating has two effects: It displaces the equilibrium toward depolymerization and it accelerates the bond breaking and reforming rate (*8*, *9*). The advantage of such reversible links is that both above-mentioned effects act together to bring fluidity and thus processability (*5*, *17*–*19*). They are, however, detrimental to the network integrity and performance. Chen *et al*. have shown that to avoid flow and creep at service temperatures, one can rely, as in thermoplastics, on glass transition to quench the system (*17*). Unfortunately, the systems based on chemical equilibrium between bond breaking and reforming are sensitive to solvents because in the presence of a solvent, the chemical equilibrium is displaced toward network depolymerization and dissolution (*19*).

We sought to show that reversible networks can flow while maintaining their integrity and insolubility at high temperature. The idea is to

Matière Molle et Chimie, UMR 7167 CNRS-ESPCI, Ecole Supérieure de Physique et Chimie Industrielles, 10 rue Vauquelin, 75005 Paris, France.

*To whom correspondence should be addressed. E-mail: ludwik.leibler@espci.fr

rely solely on exchange reactions, without the need of depolymerization-polymerization equilibria or termination reactions (Fig. 1A). The key is to design the chemistry so that at high temperature, exchange reactions enable stress relaxation and malleability and upon cooling, the exchanges become so slow that the topology of the network is essentially fixed and the system behaves like a soft solid. The reversible freezing of the topology controlled by exchange reaction kinetics will thus exhibit features of the glass transition such as cooling- and heating-rate dependence or physical aging.

To demonstrate the concept, we used the well-established transesterification reaction, which proceeds by association of all partners into an intermediate state before separation into a new partnership (*21*, *22*). We synthesized networks by classical epoxy chemistry: reaction of the diglycidyl ether of bisphenol A (DGEBA) and a mixture of fatty dicarboxylic and tricarboxylic acids. We chose the epoxy/COOH 1:1 stoichiometry to have both –OH and ester groups in the final material and checked by infrared spectroscopy the complete conversion of epoxy groups (fig. S1). Examples of transesterification reactions allowed in this system are illustrated in Fig. 1B. The transesterification kinetics can be controlled conveniently by a large variety of catalysts. Guided by a study of transterification kinetics of model molecules, we chose to work with zinc acetate [$Zn(ac)_2$] (figs. S2 to S5).

At room temperature, the cross-linked network behaves like an elastomer (figs. S6 to S9). It has a modulus of about 4 MPa and elongation and stress at break of about 180% and 9 MPa, respectively. Infrared spectroscopy indicated that the reaction is complete and that the number of ester links does not vary when the samples are heated (fig. S10). The permanence of the network was confirmed by dissolution experiments. They showed that samples swell, but do not dissolve, in good solvents even after immersion at high temperature and for a long time. Figure 2A shows swelling data for trichlorobenzene.

Rheology and birefringence studies indicated that even though the network is insoluble, it is able to completely relax stresses at high temperatures and to flow (Fig. 2B). The inset in Fig. 2B presents the temperature variation of viscosity, which follows the simple Arrhenius law with an activation energy of ~80 kJ/mol K. Notably, the stress relaxation times are about equal to exchange reaction times measured for model molecules, and so is the activation energy (fig. S5). At 100°C, the measured relaxation time is ~58 hours. Extrapolated to 40°C the value would be ~1 year, and at room temperature ~6 years.

Broken or ground samples, despite being permanently cross-linked well beyond the gel point, can be reprocessed by injection molding (Fig. 2C). By adapting the mold temperature and dwell time, molding without shrinkage can be achieved. The gradual Arrhenius-like variation of viscosity enables manufacturing techniques usually limited to a few inorganic glasses. Objects of complex shapes can be easily made without resort to a mold by local heating, deformation, relaxation of residual stresses, and welding if necessary. An elastomer fusilli made by twisting a cross-linked ribbon is shown in Fig. 2D. Because viscosity does not decrease abruptly with temperature, a precise control of temperature is not necessary, and tools such as a hot air blower are sufficient (movie S1).

The concept of exchangeable links can also be applied to design materials that are hard at room temperature and malleable but insoluble at elevated temperatures. Widely used resins made by epoxy-anhydride reactions possess hydroxy groups and ester links (*23*), and thus it is possible to take advantage of transesterification exchanges merely by adding an appropriate catalyst to classical formulations. We synthesized networks by reaction of DGEBA with glutaric anhydride with epoxy/acyl 1:1 in the presence of 5 or 10 mol% zinc acetyl acetonate [$Zn(acac)_2$]. We verified by infrared spectroscopy and swelling experiments that the network does not depolymerize even after a long time at high temperatures (fig. S11). For example, in trichlorobenzene at 180°C, once the swelling equilibrium is reached, the swelling stays constant even after 16 hours of immersion.

The material behaves like a classical hard epoxy resin with the glass transition at ~80°C (fig. S12), modulus of ~1.8 GPa (fig. S13), and stress at break of ~55 MPa at room temperature (Fig. 3A). However, in contrast to classical epoxy-anhydride resins, transesterification reactions and resulting topology rearrangements allow the network to flow. For example, at 200°C, for the network containing 10 mol% catalyst in an elongational creep experiment, after the transient

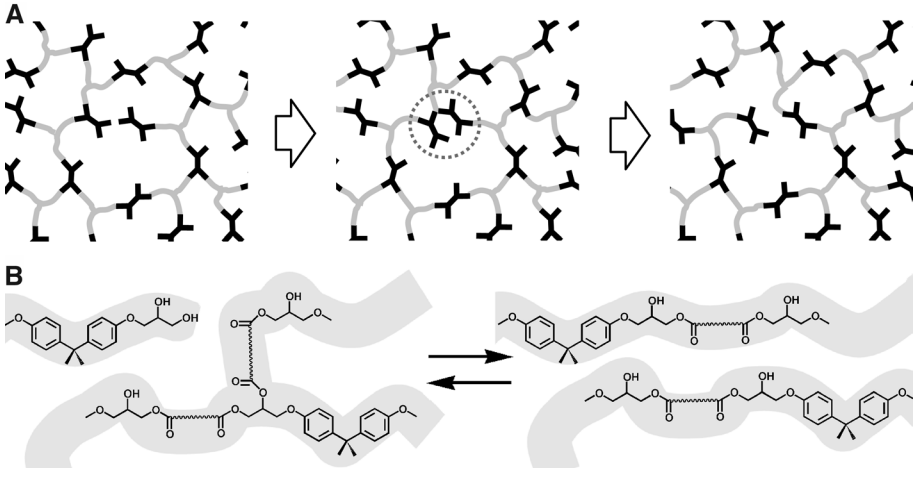

Fig. 1. Topological rearrangements via exchange reactions preserving the network integrity. (**A**) Schematic view of a network with exchange processes that preserve the total number of links and average functionality of cross-links. The middle image illustrates that the exchange does not require depolymerization in the intermediate step. (**B**) Exchange process via transesterification in hydroxy-ester networks.

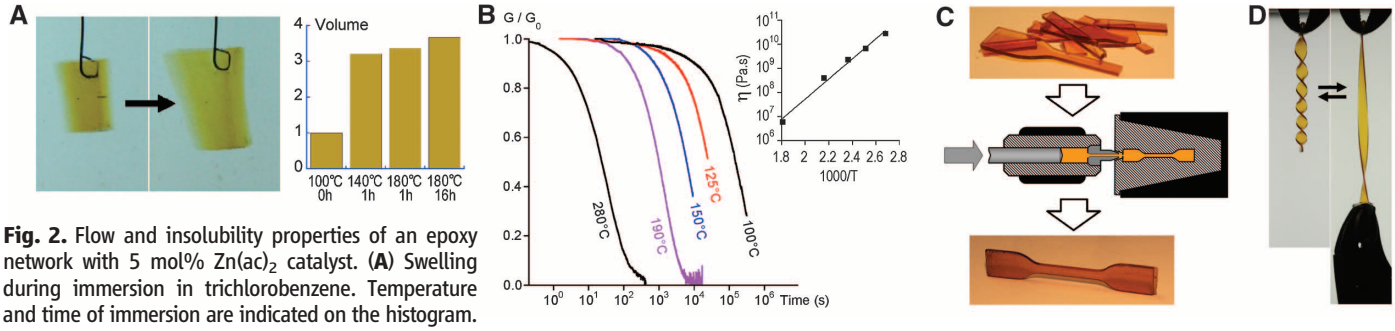

Fig. 2. Flow and insolubility properties of an epoxy network with 5 mol% $Zn(ac)_2$ catalyst. (**A**) Swelling during immersion in trichlorobenzene. Temperature and time of immersion are indicated on the histogram. (**B**) Normalized stress relaxation at different temperatures. The inset shows the temperature variation of zero-shear viscosity. (**C**) A cross-linked sample broken into pieces is reprocessed in an injection machine to recover its initial aspect and properties. No shrinkage is observed after demolding. (**D**) A fusilli-shaped elastomer made by local heating from a cross-linked ribbon of length 10 cm is reversibly deformed by a weight of 1.4 kg.

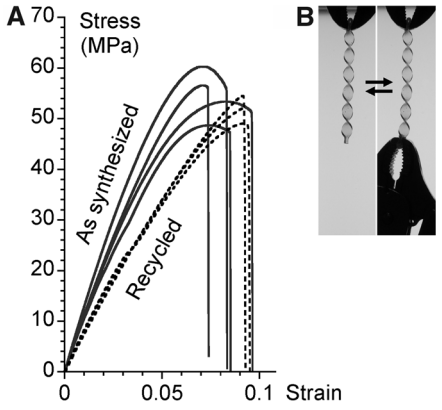

Fig. 3. Mechanical properties, malleability, and recyclability of epoxy-anhydride network with 10 mol% $Zn(acac)_2$ catalyst. (**A**) Tensile test for samples as synthesized (solid lines) and after grinding into a powder and remolding (dashed lines). (**B**) Fusilli-shaped hard thermoset made by local heating from a cross-linked ribbon of length 10 cm is practically not deformed by a weight of 1.4 kg.

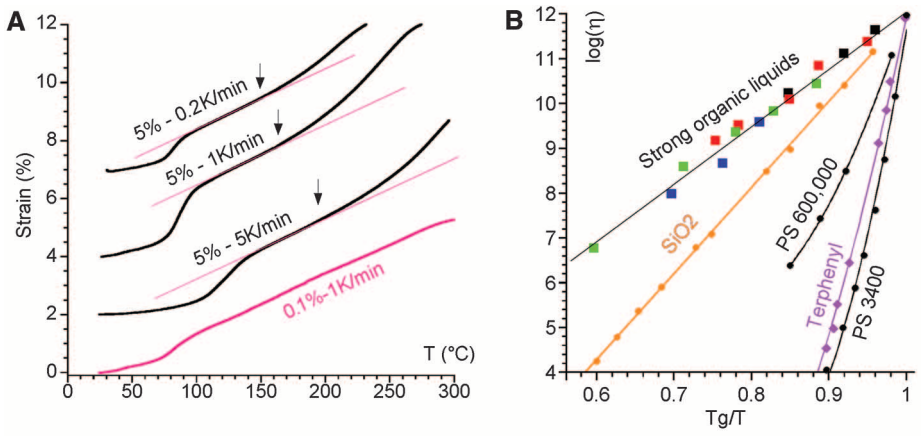

Fig. 4. Organic strong glass-former. (**A**) Temperature dependence of thermal expansion of networks with 0.1 mol % (purple) and 5 mol % $Zn(acac)_2$ (black) for various heating rates. Traces are shifted for clarity. (**B**) Angell fragility plot (*26*) showing viscosity as a function of inverse temperature normalized to 1 at the glass transition temperature (Tg) for epoxy/anhydride with 5% (red squares) and 10% (black squares) $Zn(acac)_2$; for epoxy/acid with 5% (green squares) and 10% (blue squares) $Zn(ac)_2$; and for silica (*27*), polystyrene (*28*), and terphenyl (*29*).

regime the deformation varies linearly with time. The viscosity estimated from the slope is found to be ~1.2×10^{10} Pa s. Measurements at different temperatures show an Arrhenius dependence with activation energy of ~88 kJ/mol K.

The cross-linked material that has been ground into a fine powder can be reprocessed and reshaped by compression molding at high temperature. Three minutes of molding at 240°C suffice to produce a recycled object having essentially the same mechanical properties and insolubility as the original one (Fig. 3A). Complex shapes can be wrought at high temperature without using molds. A helical fusilli-like hard epoxy object (Fig. 3B) can be made from a ribbon by successive twists and stress relaxation or by slow torsion at high temperature. Another, more conventional, method of recycling could consist of depolymerizing networks by breaking ester links through hydrolysis or alcoholysis at high temperature and pressure.

Fundamentally, at high temperatures, a network with exchangeable links behaves like a viscoelastic fluid. Yet, it differs qualitatively from polymer melts whose flow properties are mainly controlled by monomer friction. Indeed, even well above the glass transition temperature, when the monomer friction is low, the exchange reaction time can be very slow and become commensurable with the experimental time scale. In such a case, the material properties become dependent on thermal history. Thus, we anticipate, for example, that during a cooling ramp, there is a temperature at which network topology rearrangements become too sluggish to be effective. Below that temperature, the cross-links and the network topology appear to be quenched. Only on further cooling will the local monomer motions become frozen, and a classical glass transition to a hard glass will take place. Both elastomer and hard glass are liquids quenched in a metastable, out-of-equilibrium state [compare (*24*)].

Dilatometry experiments provide a classical tool (*25*) to reveal glass transitions and their thermal history dependence. Cross-linked networks are known to exhibit a lower expansion coefficient than the corresponding non–cross-linked polymers. For the sample with 0.1 mol% $Zn(acac)_2$ catalyst, the linear expansion coefficient remains constant from 50° to 250°C, as expected for a permanently cross-linked network (Fig. 4A). When more catalyst is present (5 mol%), the exchange reactions are faster and an increase in expansion coefficient is observed at a temperature of ~165°C and heating rate of 5 K/min. Notably, the transition is continuous and heating-rate dependent, as expected for a glass transition. The topology freezing transition is well separated from the glass transition, which is visible at lower temperature for both samples with and without a catalyst. Both the topology freezing (liquid-elastomer) and classical glass transition shift to higher temperatures when the heating rate is increased.

Conventionally, the liquid-to-glass transition temperature is the point at which the viscosity becomes higher than 10^{12} Pa s (*25*, *26*). For the epoxy-acid networks, viscosity studies give a transition temperature of ~68°, 57°, and 53°C for samples with 1, 5, and 10 mol% Zn catalyst, respectively. The rate of change of viscosity evaluated at the glass transition temperature (the "fragility") gives a measure of the broadness of the glass transition (*26*). Silica and a few other inorganic compounds, such as P_2O_5, show a very broad Arrhenius-like variation and are therefore called "strong" glass formers. All organic and polymer liquids are "fragile"; they show a more rapid increase of viscosity upon cooling than predicted by the Arrhenius equation (Fig. 4B). By contrast, our networks behave like silica. Because the activation energies for monomer friction and for exchange reactions are different, this topology freezing transition can occur above the classical glass transition temperature.

Macroscopically, the topology freezing transition manifests itself like a glass transition except that below the transition, the material behaves like an elastomer and not like a hard glass. The exchange reactions follow the Arrhenius law, and therefore the stress relaxation time and the viscosity also vary as predicted by the Arrhenius equation. The system can be termed a strong glass-former or strong organic liquid as opposed to strong inorganic liquids like silica and to organic glass-formers or polymers that are fragile liquids [compare (*26*)].

We have designed and realized covalently cross-linked organic networks that behave like silica. The underlying concept is to allow for reversible exchange reactions by transesterification that rearrange the network topology while keeping constant the total number of links and the average functionality of cross-links. The chemistry is versatile, relies on readily available ingredients, and does not require any special equipment. The production of malleable, reparable, recyclable and yet insoluble epoxy networks described here could potentially affect many industries that rely on elastomers, thermosetting polymers, and composites. The experimental and theoretical studies of networks with reversibly exchangeable links and a controllable number of defects could yield insights into the physics of glasses, while the control of glassy dynamics and glass transition with the catalyst is an unusual twist.

References and Notes

1. J. Ferry, *Viscoelastic Properties of Polymers* (Wiley, New York, 1980).
2. S. J. Rowan, S. J. Cantrill, G. R. L. Cousins, J. K. M. Sanders, J. F. Stoddart, *Angew. Chem. Int. Ed.* **41**, 898 (2002).
3. J.-M. Lehn, *Prog. Polym. Sci.* **30**, 814 (2005).
4. T. Maeda, H. Otsuka, A. Takahara, *Prog. Polym. Sci.* **34**, 581 (2009).

5. C. J. Kloxin, T. F. Scott, B. J. Adzima, C. N. Bowman, *Macromolecules* **43**, 2643 (2010).
6. R. J. Wojtecki, M. A. Meador, S. J. Rowan, *Nat. Mater.* **10**, 14 (2011).
7. M. S. Green, A. V. Tobolsky, *J. Chem. Phys.* **14**, 80 (1946).
8. M. Rubinstein, A. N. Semenov, *Macromolecules* **31**, 1386 (1998).
9. F. Tanaka, *Polymer Physics: Applications to Molecular Association and Thermoreversible Gelation* (Cambridge Univ. Press, Cambridge, 2011).
10. L. Leibler, M. Rubinstein, R. H. Colby, *J. Phys. II* **3**, 1581 (1993).
11. T. F. Scott, A. D. Schneider, W. D. Cook, C. N. Bowman, *Science* **308**, 1615 (2005).
12. Y. Higaki, H. Otsuka, A. Takahara, *Macromolecules* **39**, 2121 (2006).
13. R. Nicolaÿ, J. Kamada, A. van Wassen, K. Matyjaszewski, *Macromolecules* **43**, 4355 (2010).
14. H. Y. Park, C. J. Kloxin, T. F. Scott, C. N. Bowman, *Macromolecules* **43**, 10188 (2010).
15. B. Ghosh, M. W. Urban, *Science* **323**, 1458 (2009).
16. Y. Amamoto, J. Kamada, H. Otsuka, A. Takahara, K. Matyjaszewski, *Angew. Chem. Int. Ed.* **50**, 1660 (2011).
17. X. X. Chen *et al.*, *Science* **295**, 1698 (2002).
18. B. J. Adzima, H. A. Aguirre, C. J. Kloxin, T. F. Scott, C. N. Bowman, *Macromolecules* **41**, 9112 (2008).
19. Y. Zhang, A. A. Broekhuis, F. Picchioni, *Macromolecules* **42**, 1906 (2009).
20. P. Reutenauer, E. Buhler, P. J. Boul, S. J. Candau, J. M. Lehn, *Chemistry* **15**, 1893 (2009).
21. R. V. Kudryavtsev, D. N. Kursanov, *Zhurnal Obshchei Khimii* **27**, 1686 (1957).
22. J. Otera, *Chem. Rev.* **93**, 1449 (1993).
23. C. A. May, Ed., *Epoxy Resins: Chemistry and Technology* (Dekker, New York, 1988).
24. R. T. Deam, S. F. Edwards, *Philos. Trans. R. Soc. A* **280**, 317 (1976).
25. J. C. Dyre, *Rev. Mod. Phys.* **78**, 953 (2006).
26. C. A. Angell, *Science* **267**, 1924 (1995).
27. G. Urbain, Y. Bottinga, P. Richet, *Geochim. Cosmochim. Acta* **46**, 1061 (1982).
28. D. J. Plazek, V. M. O'Rourke, *J. Polym. Sci. A2 Polym. Phys.* **9**, 209 (1971).
29. D. J. Plazek, C. A. Bero, I. C. Chay, *J. Non-Cryst. Solids* **172–174**, 181 (1994).

Acknowledgments: We gratefully acknowledge helpful discussions, with H. A. H. Meijer and A. J. Ryan on polymer processing, with K. Matyjaszewski on chemical reactions and catalysis, and with F. Krzakala and A. Maggs on glass transition. We are indebted to L. Breucker and S. Abadie for help with experiments. We acknowledge funding from ESPCI, CNRS and Arkema. The authors are declared to be inventors on three patents filed by CNRS related to the work presented here: L. Leibler, D. Montarnal, F. Tournilhac, M. Capelot, FR10.54213 (2010); FR11.50888 (2011); and FR11.50546 (2011).

Supporting Online Material

www.sciencemag.org/cgi/content/full/334/6058/965/DC1
Materials and Methods
Figs. S1 to S13
Table S1
Movie S1

15 August 2011; accepted 5 October 2011
10.1126/science.1212648

Domain Dynamics During Ferroelectric Switching

Christopher T. Nelson,[1] Peng Gao,[1] Jacob R. Jokisaari,[1] Colin Heikes,[2] Carolina Adamo,[2] Alexander Melville,[2] Seung-Hyub Baek,[3] Chad M. Folkman,[3] Benjamin Winchester,[4] Yijia Gu,[4] Yuanming Liu,[5] Kui Zhang,[1] Enge Wang,[6] Jiangyu Li,[5] Long-Qing Chen,[4] Chang-Beom Eom,[3] Darrell G. Schlom,[2,7] Xiaoqing Pan[1]*

The utility of ferroelectric materials stems from the ability to nucleate and move polarized domains using an electric field. To understand the mechanisms of polarization switching, structural characterization at the nanoscale is required. We used aberration-corrected transmission electron microscopy to follow the kinetics and dynamics of ferroelectric switching at millisecond temporal and subangstrom spatial resolution in an epitaxial bilayer of an antiferromagnetic ferroelectric ($BiFeO_3$) on a ferromagnetic electrode ($La_{0.7}Sr_{0.3}MnO_3$). We observed localized nucleation events at the electrode interface, domain wall pinning on point defects, and the formation of ferroelectric domains localized to the ferroelectric and ferromagnetic interface. These results show how defects and interfaces impede full ferroelectric switching of a thin film.

Ferroelectric materials have numerous applications, including high-density and nonvolatile memories (*1*–*3*) and a broad range of electronic, optical, and acoustic devices (*2*). The utility of ferroelectrics is derived from a reversible transition between equivalent polar orientation states under an applied electric field and from that transition's coupling to other material properties including strain (*4*, *5*), magnetic order (*6*), and surface charge (*7*). Most of these applications require low-dimensional geometries such as thin films and deterministic control of the local polarization state at the interface (*8*). Thus, it is critical to understand the process of polarization switching in epitaxial thin films.

In this work, we studied the domain nucleation and evolution during switching of a ferroelectric $BiFeO_3$ thin film, using in situ structural characterization by transmission electron microscopy (TEM). Polarization switching is induced by an applied electric field oriented along the film normal between a surface probe and a planar bottom electrode, the same geometry used for surface probe characterization depicted schematically in Fig. 1. Ferroelectric switching occurs through a process of inhomogenous nucleation and anisotropic growth of favorably oriented domains (*9*). In this geometry, it is typically modeled by a single nucleation event occurring at the probe contact with the film surface, the maximum of the applied field, followed by rapid propagation of the nucleated domain across the film and slow lateral growth (see simulation in fig. S1 and movie S1). The creep-type lateral expansion stage is well known for switching in thin films from surface probe measurements (*10*) and modeling (*11*); however, experimental observations of the initial normal-axis growth process are absent except at much larger length scales (*12*, *13*). In this work, we followed domain nucleation and evolution in cross-section and directly observed inhomogeneous nucleation events, domain wall pinning, and the formation of ferroelectric domains localized at interfaces.

Local switching of a 100-nm $(001)_P$ oriented $BiFeO_3$ ferroelectric film was performed by applying an electrical bias between an etched tungsten surface probe and a 20-nm $La_{0.7}Sr_{0.3}MnO_3$ buffer electrode. This bilayer was grown on closely lattice-matched single-crystal $(110)_O$ $TbScO_3$ substrates (compressive strain <0.14%) to avoid instabilities from epitaxial strain (*14*) and misfit dislocations (*15*) or flexoelectric effects from strain gradients (*16*) (O indicates orthorhombic indices and P indicates pseudocubic, where $[110]_O \parallel [001]_P$). The bias between the surface probe and buffer electrode results in an inhomogenous out-of-plane electric field in the $BiFeO_3$ film, promoting a transition among the eight possible $<111>_P$ polarization directions between the four "up" and four "down" orientation states. Three types of switching are possible, classified by the angular rotation of the polarization vector during swiching: 71°, 109°, or 180°. We find that the preferred switching path is the 71° rotation of the spontaneous polarization by the reversal of only the polarization component parallel to the applied field, in this case the film normal (*z* axis), in agreement with other studies (*17*–*19*). Piezoresponse force microscopy (PFM) indicates that the as-grown $BiFeO_3$ films are predominantly upward-poled. Figure 1A shows an out-of-plane PFM phase image from a 100-nm $BiFeO_3$ film, which was locally switched by a positive probe bias of 20.6 V with a 2-s dwell time, producing a downward-poled domain ~400 nm in diameter.

Diffraction contrast TEM was used to resolve the evolution of the domain structure along the depth of the film in situ. A cross-section of the 100-nm $BiFeO_3$ film measured by PFM was

[1]Department of Materials Science and Engineering, University of Michigan, Ann Arbor, MI 48109, USA. [2]Department of Materials Science and Engineering, Cornell University, Ithaca, NY 14853, USA. [3]Department of Materials Science and Engineering, University of Wisconsin–Madison, Madison, WI 53706, USA. [4]Department of Materials Science and Engineering, Penn State University, University Park, PA 16802, USA. [5]Department of Mechanical Engineering, University of Washington, Seattle, WA 98195, USA. [6]School of Physics, Peking University, Beijing 100871, China. [7]Kavli Institute at Cornell for Nanoscale Science, Ithaca, NY 14853, USA.

*To whom correspondence should be addressed. E-mail: panx@umich.edu